Bulletin of Faculty of Pharmacy, Cairo University (2014) **52**, 103–108

Cairo University

Faculty of Pharmacy

Cairo University

Bulletin of Faculty of Pharmacy, Cairo University

www.elsevier.com/locate/bfopcu
www.sciencedirect.com

ORIGINAL ARTICLE

Pharmacophore mapping: Prediction of BCR–ABL kinase inhibitory activity of α-benzylthio chalcones

Richa Bajaj, Vikas Sharma, Vipin Kumar *

Institute of Pharmaceutical Sciences, Kurukshetra University, Kurukshetra 136119, Haryana, India

Received 28 August 2013; accepted 17 October 2013
Available online 23 November 2013

KEYWORDS

Chalcone;
Anticancer activity;
3D-QSAR;
Pharmacophore hypothesis;
Regression coefficient

Abstract In this investigation, 3D pharmacophore modeling studies were performed on a diverse set of 33 α-benzylthio chalcone derivatives that demonstrate anticancer activity by blocking BCR–ABL phosphorylation in leukemic cells. Pharmacophore modeling is based on the principle of the alignment of pharmacophoric features which has been carried out on the same set of molecules. Five point pharmacophores with one negative ionizable group, one hydrophobic group and three aromatic rings as pharmacophoric features were developed. Pharmacophore hypothesis HNRRR 1501 yielded a statistically significant 3D-QSAR model with R^2 value 0.9103 and was considered to be the best pharmacophore hypothesis. The selected pharmacophore model HNRRR 1501 was externally validated by predicting the activity of test set. The correlation coefficient of 0.8856 was observed between experimental and predicted activities of test set. The features of pharmacophore were expected to be useful for the design of selective BCR–ABL tyrosine kinase inhibitors.

1. Introduction

Chronic myelogenous leukemia (CML) is a slow growing cancer where white blood cells are produced in excess by bone marrow.[1] In Chronic myelogenous leukemia patients, the reciprocal translocation between the long arms of chromosomes 9 and 22, results in the Philadelphia (Ph1) chromosome.[2,3] As evident from *in vitro* and *in vivo* studies, it has been established that the tyrosine kinase activity of the BCR–ABL is sufficient to cause CML,[4–7] which makes BCR–ABL tyrosine kinase inhibitors as the first line therapy for CML.[8] BCR–ABL tyrosine kinase inhibitors inhibit the expression of specific target genes that contribute to the malignant transformation of Philadelphia positive cells.[9]

Traditional natural products have cancer preventing properties.[10] In a recent review, Sharma et al. described the potential of heterocyclic chalcone analogs as potential anticancer agents.[11] The effectiveness of chalcone derivatives in different cancers is proved by various researchers from time to time i.e. leukemia, colorectal adenocarcinoma, melanoma,[12] cervical carcinoma, breast cancer, lung carcinoma,[13] colon

* Corresponding author. Tel.: +91 1744 239617.
E-mail addresses: richa_bajaj4@yahoo.com (R. Bajaj), vikas_pharma@rediffmail.com (V. Sharma), vipbhardwaj@rediffmail.com (V. Kumar).

Peer review under responsibility of Faculty of Pharmacy, Cairo University.

ELSEVIER Production and hosting by Elsevier

 http://dx.doi.org/10.1016/j.bfopcu.2013.10.001

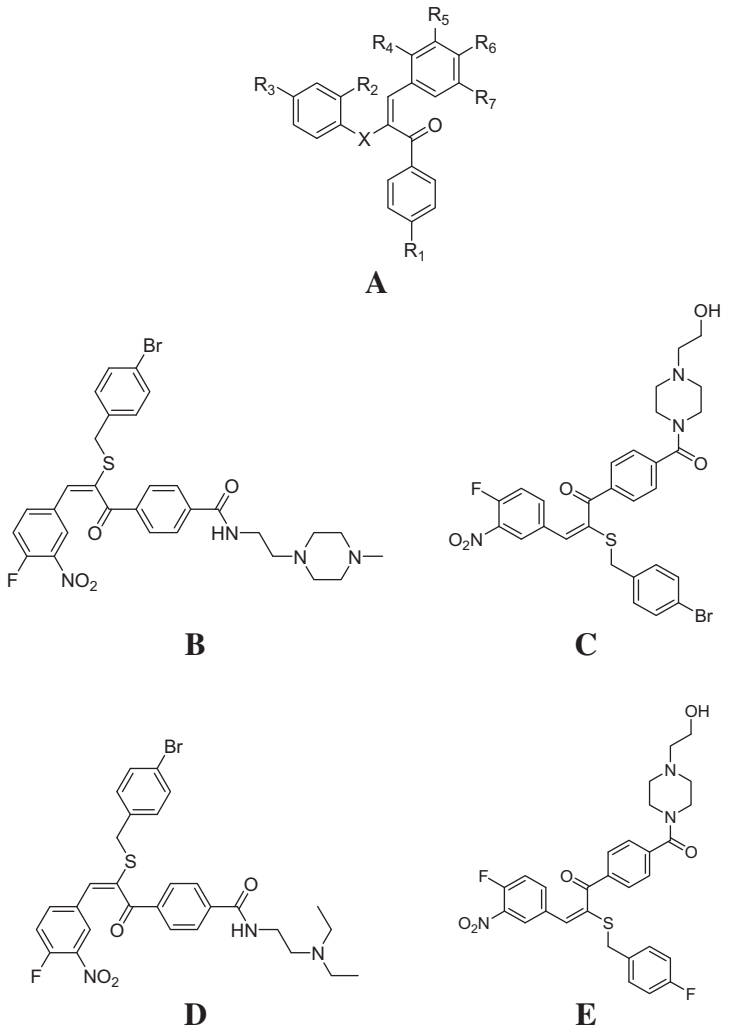

Figure 1 Basic structures of chalcone series.

cancer,[14,15] chronic myelogenous leukemia,[16] and prostate cancer.[17] *α-benzylthio chalcone was discovered as a new class of BCR–ABL tyrosine kinase inhibitors* that exhibit cytotoxicity against leukemia (K562) cells.[16]

3D-QSAR is a quantitative correlation between structure and experimental activity of the compounds.[18] 3D-QSAR model is developed by using three dimensional conformers of active compounds and score a compound on the basis of fitting function that evaluate the alignment of three dimensional chemical features (hydrogen donor, hydrogen acceptor, hydrophobic groups, chargeable group, and aromatic rings) of the model.[19] The activity of new compounds can be quantitatively predicted by evaluating how well each compound maps onto the pharmacophore model.[20]

In the present study, pharmacophore models have been generated and validated for the prediction of BCR–ABL tyrosine kinase inhibitory activity of α-benzylthio chalcone derivatives using the PHASE module of Schrodinger suite. The alignment obtained from the pharmacophoric points is used to derive a pharmacophore based 3D-QSAR model.[20]

2. Experimental

2.1. Dataset

A series of 33 α-benzylthio chalcone derivatives having BCR–ABL kinase inhibitory activity in leukemic K562 cells was used for the present studies.[16] The IC_{50} values of BCR–ABL kinase inhibitory activity were converted to pIC_{50}. Dataset was divided randomly into training and test set by considering the 50% of the total molecules in the training set (seventeen molecules) and 50% in the test set (sixteen molecules). Training set was used to generate pharmacophore models and the proposed models were validated by predicting the activity of test set molecules. The basic structure for chalcone derivatives is depicted in Fig. 1 and various substituents are enlisted in Table 1.

2.2. Pharmacophore modeling

In the present work, PHASE[21] software has been used to generate pharmacophore models. The structures of all the training set molecules were drawn using maestro[22] and then subjected

Table 1 BCR–ABL kinase inhibitory activity of α-benzylthio chalcones.

Comp. No.	Series	R_1	R_2	R_3	R_4	R_5	R_6	R_7	X	Set
1	A	COOH	H	Br	H	NO_2	Cl	H	CH_2S	Training
2	A	COOH	H	Br	H	NO_2	Br	H	CH_2S	Training
3	A	COOH	H	Br	H	NO_2	F	H	CH_2S	Test
4	A	COOH	H	Cl	H	NO_2	F	H	CH_2S	Training
5	A	COOH	H	Cl	H	NO_2	Cl	H	CH_2S	Test
6	A	COOH	H	Cl	H	NO_2	Br	H	CH_2S	Test
7	A	COOH	H	F	H	NO_2	Cl	H	CH_2S	Training
8	A	COOH	H	F	H	NO_2	F	H	CH_2S	Training
9	A	COOH	H	F	H	NO_2	Br	H	CH_2S	Test
10	A	F	H	F	H	NO_2	F	H	CH_2S	Training
11	A	COOH	H	F	H	NO_2	Cl	H	CH_2S	Test
12	A	COOH	F	F	H	NO_2	F	H	CH_2S	Test
13	A	COOH	Cl	Cl	H	NO_2	Cl	H	CH_2S	Training
14	A	COOH	Cl	Cl	H	NO_2	F	H	CH_2S	Test
15	A	COOH	Cl	Cl	H	NO_2	Br	H	CH_2S	Test
16	A	COOH	Cl	Cl	H	NO_2	F	H	CH_2S	Training
17	A	COOH	H	CH_3	H	NO_2	F	H	CH_2S	Training
18	A	COOH	H	Br	H	NO_2	F	H	CH_2S	Test
19	A	COOH	H	H	H	NO_2	F	H	CH_2SO_2	Test
20	A	COOH	H	Br	H	NO_2	F	H	CH_2SO_2	Test
21	A	COOH	H	Br	H	NO_2	Cl	H	CH_2SO_2	Training
22	A	COOH	H	Br	H	NO_2	F	H	S	Test
23	A	COOH	H	Br	H	OCH_3	F	H	CH_2S	Training
24	A	COOH	H	Br	H	Br	OH	H	CH_2S	Training
25	A	COOH	H	Br	H	NO_2	OH	H	CH_2S	Test
26	A	COOH	H	Br	F	H	H	NO_2	CH_2S	Training
27	A	COOH	H	Br	H	F	NO_2	H	CH_2S	Test
28	A	COOH	H	Br	NO_2	H	F	H	CH_2S	Test
29	A	COOH	H	Br	F	H	NO_2	H	CH_2S	Training
30	B	–	–	–	–	–	–	–	–	Training
31	C	–	–	–	–	–	–	–	–	Training
32	D	–	–	–	–	–	–	–	–	Test
33	E	–	–	–	–	–	–	–	–	Training

Table 2 Parameters of five featured pharmacophore hypothesis.

Sr. No.	Hypothesis	Survival score	R^2	F	Q^2	RMSD
1	HNRRR 1501	20.671	0.91	146	0.71	0.4
2	HNRRR 1507	20.604	0.7949	65.9	0.519	0.54
3	HNRRR 2909	20.604	0.7221	44	0.49	0.62

to LigPrep program which produces high-quality, all-atom 3D structures with correct chiralities for each proposed input structure. All the structures were ionized at neutral pH 7. Conformers were generated with the Monte Carlo method by optimized potential for liquid simulations (OPLS-2005) force field with implicit GB/SA distance-dependent dielectric solvent model at cutoff root mean square deviation (RMSD) of 1 (MacroModel 9.6 2010) with 1000 iterations using water as the solvent. All the conformers were subsequently minimized using Truncated Newton Conjugate Gradient (TNCG) minimization up to 500 interactions. A conformer set for each molecule with a maximum energy difference of 30 kcal/mol relative to the global energy minimum conformers was preserved.[21,22]

In the next step for the development of pharmacophore model, a set of pharmacophoric features namely aromatic ring (R), hydrogen bond acceptor (A) and hydrophobic groups (H)

Table 3 Distances between different sites of model HNRRR 1501.

Site1	Site2	Distance (Å)	Site1	Site2	Distance (Å)
H6	N7	7.073	N7	R10	3.532
H6	R8	5.093	R8	R9	9.422
H6	R9	4.417	R8	R10	6.822
H6	R10	3.655	R9	R10	5.893
N7	R8	9.043	N7	R9	8.903

Table 4 Angles between different sites of model HNRRR 1501.

Site1	Site2	Site3	Angle (°)	Site1	Site2	Site3	Angle (°)
R8	H6	R9	164.3	N7	R8	R9	57.6
R8	H6	R10	101.2	N7	R8	R10	20.1
R9	H6	R10	93.3	R9	R8	R10	20.1
N7	H6	R8	94.6	H6	R9	N7	51.7
N7	H6	R9	98.9	H6	R9	R8	8.4
N7	H6	R10	10.0	H6	R9	R10	38.3
H6	N7	R8	34.2	N7	R9	R8	59.1
H6	N7	R9	29.3	N7	R9	R10	14.7
H6	N7	R10	10.4	R8	R9	R10	46.1
R8	N7	R9	63.3	H6	R10	N7	159.6
R8	N7	R10	41.7	H6	R10	R8	47.1
R9	N7	R9	25.0	H6	R10	R9	48.4
H6	R8	N7	51.2	N7	R10	R8	118.2
H6	R8	R9	7.3	N7	R10	R9	140.3
H6	R8	R10	31.7	R8	R10	R9	95.4

Table 5 Experimental and predicted pK_i values of training set molecules based on hypothesis HNRRR 1501.

Comp No.	Experimental pK_i	Predicted pK_i	Fitness score	Comp No.	Experimental pK_i	Predicted pK_i	Fitness score
1	6.154	5.87	1.62	21	4.602	4.88	1.58
2	6.045	5.79	1.59	23	6.221	5.99	1.53
4	6. 1	6.03	1.79	24	6.698	6.72	1.60
7	6.301	5.87	1.61	26	6.522	6.70	1.59
8	6.397	6.60	2.94	29	4.124	4.45	1.59
10	6.221	6.48	2.91	30	5.124	5.24	1.59
13	6.221	6.58	2.92	31	5.301	4.98	1.59
16	6.522	6.62	3.00	33	5.124	4.98	1.68
17	6.397	6.52	2.91				

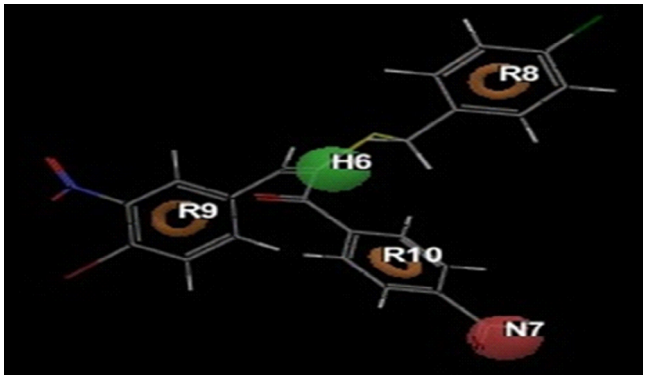

Figure 2 Hypothesis HNRRR 1501 aligned with representative compound 8. Pharmacophore features are coded: negative ionizable group (N7), hydrophobic (H6), and three aromatic rings (R8, R9, R10).

was used to create pharmacophore sites for all the prepared ligands that could effectively map all critical chemical features of dataset molecules. Minimum and maximum number of sites for all the features were 3 and 6, respectively. Pharmacophore matching tolerance was set to 1 Å. Hypotheses were generated by a systematic variation of number of sites and the number of matching active compounds. These selected features were used to build a series of hypotheses by selecting *find the common pharmacophore* option in PHASE. Common pharmacophores are identified using a tree-based partitioning technique that groups together similar pharmacophores according to their inter site distances. The regression analysis was performed by constructing a series of models with an increasing number of

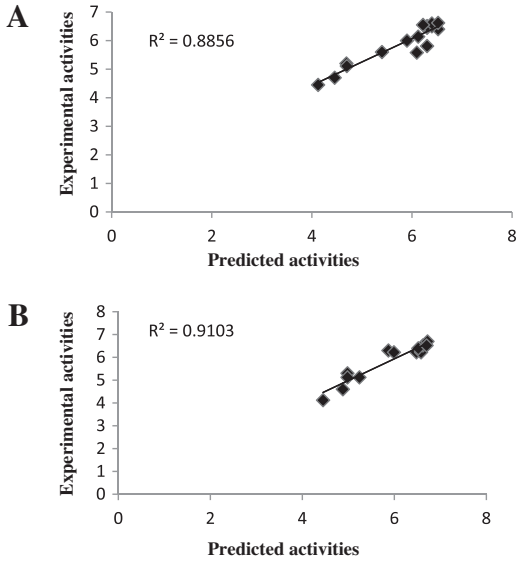

Figure 3 Relationship between experimental and HNRRR 1501 predicted BCR–ABL tyrosine kinase inhibitory activity of test set (A) and training set (B) molecules.

PLS factors. 3D-QSAR models were generated for the hypotheses using 18 molecules of training set with one to three PLS factors and a grid spacing of 1 Å. The model partitions space into a grid of uniformly sized cubes. Cubes occupied by the atoms of each class correspond to a ligand, represented by a set of bit values (0 or 1). These binary-values were used to develop a correlation with biological activity. Further, common pharmacophore hypotheses were examined using the survival score to yield the best alignment of the active ligands using an overall maximum root mean square deviation (RMSD) value of 1.2 Å for distance tolerance. The hypotheses were scored using default parameters for site, vector, volume, number of matches, selectivity and energy terms. Survival score secured by each hypothesis, is the measure of the quality of alignment for a particular hypothesis.[20,23]

2.3. Validation of pharmacophore model

Validation is considered to be a conclusive proof to assess the predictability of a model. Our priority was to develop a pharmacophore model that can predict the activity of the molecules accurately, and it should identify active compounds from a dataset. In the present study, the prediction of the activity of test set molecules was used as a method to validate the developed pharmacophore model. All the test set molecules were processed similar to the training set molecules, and then the activities of test set molecules were predicted using the developed pharmacophore model. The correlation between the experimental and predicted activities of the test set molecules was then determined.

3. Results and discussion

BCR–ABL tyrosine kinase activity is essential for the transforming function of the protein. A well-known aspect of BCR–ABL transformation is its ability to activate multiple signaling pathways that lead to proliferation, reduced growth factor-dependence and apoptosis, and abnormal interaction with extra-cellular matrix. Previous reports suggest that the suppression of apoptosis constitutes an important mechanism by which BCR–ABL drives the expansion of myeloid cells.[24–26]

Ligand-based drug design relies on the knowledge of known molecules possessing pharmacological activity that bind to the biological target of interest. These α-benzylthio chalcone derivatives may be used to derive a pharmacophore which defines the minimum necessary structural characteristics a molecule must possess in order to bind to the target.[27] Ligand based approaches consider two or three dimensional shape, chemistry, and pharmacophoric points to assess similarity. Ligand based QSAR approaches require a number of active molecules having a wide range of activities against target receptor.[28]

Seventeen molecules forming the training set were used to develop the pharmacophore models. Selected features (pharmacophoric) for creating sites were hydrogen bond acceptor (A), hydrophobic group (H), aromatic ring (R), hydrogen bond donor (D), and negatively ionizable group (N). Pharmacophore models containing three to six features were generated. Pharmacophore hypotheses with five features were selected (Table 2) and subjected to stringent scoring function analysis.

HNRRR1501 is the best hypothesis in this study characterized by the highest survival score, highest F value and the best regression coefficient (0.9103). The features represented by this hypothesis are, one hydrophobic group (H), one negative ionizable group (N) and three aromatic rings (R). The distances and angles between different sites of HNRRR 1501 are given in Table 3 and Table 4, respectively. For each ligand, one aligned conformer based on the lowest RMSD of feature atom coordinates from those of the corresponding reference feature was superimposed on HNRRR 1501. The fitness scores for all ligands were observed on model HNRRR 1501. The activity of a compound corresponds with its fitness score i.e. high fitness score indicates more activity prediction for a compound.[20] Besides checking mapping of a feature, fit function also measures the distance between the features of a molecule with respect to features of the hypothesis.[20] Table 5 shows the fitness score for all the molecules of training set. Fig. 2 shows Hypothesis HNRRR 1501 aligned with representative molecule 8 (pIC_{50} = 6.397) of the training set.

Another validation method to characterize the quality of HNRRR 1501 is represented by its capacity for correct activity prediction of training set molecules. The actual and predicted BCR–ABL tyrosine kinase inhibitory activity of training set molecules on the pharmacophore hypothesis HNRRR 1501 are shown in Table 5. The predicted BCR–ABL tyrosine kinase inhibitory activity of training set molecules exhibited a correlation of 0.9103 with a reported BCR–ABL tyrosine kinase inhibitory activity using model HNRRR 1501 (Fig. 3). In addition to this survival score analysis and prediction of activity of training set molecules, the validity of the pharmacophore model HNRRR 1501 was further assessed by predicting test set activity. Like training set molecules, test set molecules were also built, minimized and used in conformational analysis. Actual and predicted activity values of test set molecules are given in Table 6. The predicted BCR–ABL tyrosine kinase inhibitory activity of test set molecules exhibited a correlation of 0.8856 with an experimental BCR–ABL tyrosine kinase inhibitory activity using model HNRRR 1501 (Fig. 3). The re-

Table 6 Experimental and predicted pK_i of test set molecules based on hypothesis HNRRR1501.

Comp. No.	Experimental pK_i	Predicted pK_i	Fitness score	Comp. No.	Experimental pK_i	Predicted pK_i	Fitness score
3	6.522	5.62	1.77	18	6.522	6.62	3.00
5	6.301	5.81	1.62	19	5.4	5.11	2.93
6	6.301	6.45	2.94	20	5.9	6.00	2.30
9	6.397	6.50	2.89	22	6.124	6.14	2.53
11	6.096	5.58	1.81	25	4.69	4.69	1.79
12	6.301	6.51	2.91	27	4.455	4.70	1.83
14	6.397	6.60	2.97	28	4.124	4.45	1.78
15	6.221	6.55	2.91	32	4.698	5.11	1.66

sults of this study revealed that model HNRRR 1501 can be used for the prediction of BCR–ABL tyrosine kinase inhibitory activity, as for a reliable model, the squared predictive correlation coefficient should be >0.6.[29,30]

4. Conclusion

This study shows the generation of a pharmacophore model HNRRR 1501 for α-benzylthio chalcones acting as BCR–ABL tyrosine kinase inhibitor. Hypothesis HNRRR 1501 represents the best pharmacophore model for determining BCR–ABL tyrosine kinase inhibitor activity. HNRRR 1501 consists of one hydrophobic group, one negative ionizable group and three aromatic ring features. This pharmacophore model was able to predict the BCR–ABL tyrosine kinase inhibitory activity and the validation results also provide an additional confidence in the proposed pharmacophore model. Results suggested that the proposed HNRRR 1501 model can be useful to rationally design and identify the new α-benzylthio chalcones as BCR–ABL tyrosine kinase inhibitor in large 3D database of molecules.

5. Conflict of interest

None.

References

1. Zhou T, Parillon L, Wang Y, Keats J, Lamore S, Xu Q, et al. Crystal structure of the T315I mutant of Abl kinase. *Chem Biol Drug Des* 2007;**70**:171–81.
2. Jabbour E, Jones D, Kantarjian HM, O'Brien S, Tam C, Koller C, et al. Long-term outcome of patients with chronic myeloid leukemia treated with second-generation tyrosine kinase inhibitors after imatinib failure is predicted by the in vitro sensitivity of BCR–ABL kinase domain mutations. *Blood* 2009;**114**:2037–43.
3. Nowakowska Z. A review of anti-infective and anti-inflammatory chalcones. *Eur J Med Chem* 2007;**42**:125–37.
4. Daley GQ, Van Etten RA, Baltimore D. Induction of chronic myelogenous leukemia: current status and investigational options. *Science* 1990;**247**:824–30.
5. Kelliher MA, McLaughlin J, Witte ON, Rosenberg N. Induction of a chronic myelogenous leukemia-like syndrome in mice with v-abl and BCR/ABL. *Proc Natl Acad Sci USA* 1990;**87**:6649–53.
6. Heisterkamp N, Jenster G, Ten Hoeve J, Zovich D, Pattengale J, Groffen J. Acute leukaemia in bcr/abl transgenic mice. *Nature* 1990;**344**:251–3.
7. Lugo TG, Pendergast AM, Muller AJ, Witte ON. Tyrosine kinase activity and transformation potency of BCR–ABL oncogene products. *Science* 1990;**247**:1079–82.
8. Lopez S, Castelli MV, Zacchino SA, Domínguez JN, Lobo G, Charris-Charris J, et al. In vitro antifungal evaluation and structure–activity relationships of a new series of chalcone derivatives and synthetic analogues, with inhibitory properties against polymers of the fungal cell wall. *Bioorg Med Chem* 2001;**9**:1999–2013.
9. Deininger MWN, Vieira S, Mendiola R, Schultheis B, Goldman JV, Melo JV. BCR–ABL tyrosine kinase activity regulates the expression of multiple genes implicated in the pathogenesis of chronic myeloid leukemia. *Cancer Res* 2000;**60**:2049–55.
10. Aggarwal BB, Shishodia S. Molecular targets of dietary agents for prevention and therapy of cancer. *Biochem Pharmacol* 2006;**71**:1397–421.
11. Sharma V, Kumar V, Kumar P. Heterocyclic chalcone analogues as potential anticancer agents. *Anticancer Agents Med Chem* 2012;**13**:422–32.
12. Avila HP, Smania EFA, Monache FD, Smania AJ. Structure–activity relationship of antibacterial chalcones. *Bioorg Med Chem* 2008;**16**:9790–4.
13. Ferrer R, Lobo G, Gamboa N, Abramjuk C, Jung K, Michael L, et al. Synthesis of (7-chloroquinolin-4-yl) amino chalcones: potential antimalarial and anticancer agents. *Sci Pharm* 2009;**77**:725–41.
14. Modzelewska A, Pettit C, Achanta G, Davidson NE, Huang P, Khan SR. Anticancer activities of novel chalcone and bis-chalcone derivatives. *Bioorg Med Chem* 2006;**14**:3491–5.
15. Achanta G, Modzelewska A, Feng L, Khan SR, Huang P. A boronic-chalcone derivative exhibits potent anticancer activity through inhibition of the proteasome. *Mol Pharmacol* 2006;**70**:426–33.
16. Ramana Reddy MV, Pallela VR, Cosenza SC, Mallireddigari MR, Patti R, Bonagura M, et al. *Bioorg Med Chem* 2010;**18**:2317–26.
17. Szliszka E, Czuba ZP, Mazur B, Paradysz A, Krol W. Chalcones and dihydrochalcones augment TRAIL-mediated apoptosis in prostate cancer cells. *Molecules* 2010;**15**:5336–53.
18. Hansch C, Sammes PG, Ramsden CA. *Quantitative drug design (comprehensive medicinal chemistry)*. New York: Pregamon Press; 1990 p. 497–560.
19. Zhang N, Ziang Y, Zou J, Zhang B, Jin H, Wang Y, et al. 3D QSAR for GSK-3β inhibition by indirubin analogues. *Eur J Med Chem* 2006;**41**:373–8.
20. Rani P, Kumar V. Development of pharmacophore models for predicting HIV-1 reverse transcriptase inhibitory activity of pyridinone derivatives. *Pharm Chem J* 2011;**45**:36–42.
21. PHASE, Version 3.0, Schrodinger LLC., NY2008.
22. Maestro, Version 8.5, Schrodinger LLC., NY2008.
23. Kumar V, Kumar S, Rani P. Pharmacophore modeling and 3D-QSAR studies on flavonoids as α-glucosidase inhibitors. *Der Pharma Chemica* 2010;**2**:324–35.
24. Druker BJ, Tamura S, Buchdunger E, Ohno S, Segal GM, Fanning S, et al. Effects of a selective inhibitor of the Abl tyrosine kinase on the growth of Bcr–Abl positive cells. *Nat Med* 1996;**2**:561–6.
25. Gambacorti-Passerini C, Le Coutre P, Mologni L, Fanelli M, Bertazzoli C, Marchesi E, et al. Inhibition of the ABL Kinase activity blocks the proliferation of BCR/ABL + leukemic cells and induces apoptosis. *Blood Cells Mol Dis* 1997;**23**:380–94.
26. Patel D, Suthar MP, Patel V, Singh R. BCR–ABL kinase inhibitors for cancer therapy. *Int J Pharm Sci Drug Res* 2010;**2**:80–90.
27. Güner Osman F. Pharmacophore: Perception, Development, and Use in Drug Design. vol. 2. La Jolla, Callif: International University Line; 2000.
28. Sharma A, Kumar V. Pharmacophore modeling and 3D QSAR studies on N-(2-benzoylphenyl)-L-tyrosines as PPARγ agonists. *J Pharm Res* 2011;**4**:1927–30.
29. Dureja H, Kumar V, Gupta S, Madan AK. Topochemical models for the prediction of lipophilicity of 1,3-disubstituted propan-2-one analogs. *J Theo Comput Chem* 2007;**6**:435–48.
30. Wold S. Validation of QSAR's. *Quant Struct Activ Relat* 1991;**10**:191–3.